Passive Wi-Fi-based Radars with 802.11ax MU-MIMO Signals: AoD Estimation with a Single Antenna

Hasan Can Yildirim*†, Laurent Storrer*, Martin Willame*†, Jérôme Louveaux†, Philippe De Doncker*, François Horlin*
*Université Libre de Bruxelles - †Université Catholique de Louvain

{*hasan.can.yildirim,laurent.storrer*}*@ulb.be*, {*martin.willame,jerome.louveaux*}*@uclouvain.be*,
{*pdedonck,fhorlin*}*@ulb.ac.be*

2023 IEEE 3rd International Symposium on Joint Communications & Sensing (JC&S) | 979-8-3503-4568-1/23/$31.00 ©2023 IEEE | DOI: 10.1109/JCS57290.2023.10107509

***Abstract*—Passive Wi-Fi based Radar (PWR) is a device that makes use of existing Wi-Fi signals to detect/track targets in the environment. Therefore, the radar processing at the PWR largely depends on the Wi-Fi signal and its characteristics. In the latest amendment of the Wi-Fi standard, namely 802.11ax, Multi-User Multiple-Input Multiple-Output (MU-MIMO) technology is used to improve the spatial efficiency of the wireless channel by precoding the transmitted signal for each user. However, from the PWR perspective, precoding affects the signal power that illuminates a given target depending on its Angle-of-Departure (AoD). In this paper, we first quantify the impact of precoded signals on PWR processing. Then, we show that it is possible to recover the AoD of well-illuminated targets by using a PWR equipped with a single-antenna. To do so, a three-step-scheme, which works by exploiting the MU-MIMO synchronization and precoded signal transmission, is proposed. The accuracy of the proposed method, as well as its shortcomings are shown through numerical analyses.**

***Index Terms*—Passive Wi-Fi Radar, MU-MIMO, precoding, angle-of-departure estimation**

I. Introduction

Passive Wi-Fi based Radars (PWRs) are devices that make use of existing Wi-Fi signals for detecting and tracking targets in an environment [1]. When the Wi-Fi signals transmitted by an Access Point (AP) reflect from the objects/targets, they become the surveillance signal, which is collected by the PWR to apply appropriate processing for target detection/tracking.

Meanwhile, the Wi-Fi standard evolves as the research progresses on various fields, and a new amendment is introduced to the standard in every few years. The most recent amendment, 802.11ax, is specifically designed to improve the Wi-Fi traffic issues by using multi-user technologies in both downlink and uplink over space and frequency domains: Multi-User Multiple-Input Multiple-Output (MU-MIMO) and Orthogonal Frequency-Division Multiple-Access, respectively [2]. Since the introduction of 802.11ax, the interest in PWRs has significantly increased [3]. This new interest rises due to the wider bandwidths available to exploit and the increased availability of Wi-Fi signals thanks to the dense deployment scenarios enabled in 802.11ax.

978-1-6654-0579-9/22/$31.00 ©202 1 IEEE

However, it is clear that the PWR processing has to be adapted to the new technologies introduced in the Wi-Fi standard so that the Wi-Fi signals can be fully exploited. Among these technologies, MU-MIMO plays a crucial role and its impact on the PWR processing is not yet addressed. In MU-MIMO the Wi-Fi AP forms directive radio waves towards different client devices (i.e., stations or STAs). To do so, an 802.11ax AP starts the Channel Sounding Session (CSS) by isotropically transmitting the priorly known Null Data Packet (NDP) [2]. Then, the STAs can estimate their wireless channel coefficients based on the received NDP and send these coefficients back to the AP. Thanks to the available explicit feedback, the AP can compute a precoding matrix and start the MU-MIMO data transmission where the interference between the STAs is minimized. Hence, from the PWR perspective, the scene which contains potential targets is globally illuminated during CSS while MU-MIMO illuminates only the vicinity of STAs.

In our previous analyses [4], we have shown that the PWR coverage is significantly altered due to the precoded Wi-Fi signals. More specifically, the Signal-to-Noise-Ratio (SNR) per target is improved in the vicinity of STAs, while it is drastically deteriorated in the remaining parts of the scene. Moreover, the precoding affects the form of the surveillance signal such that the surveillance signal is no longer the product between the channel coefficients and the transmitted symbols in the frequency domain. This is only because that Wi-Fi signals are precoded to match a specific set of channel coefficients –those of the STAs. Therefore, the targets that are not closely located with the STAs will be illuminated by a signal which is the aggregation of its channel coefficients, the precoder, and the data for each STA. In other words, the surveillance signal received after bouncing on a target will not only depend on the target location and movement, but also on the geometry of the communication channel, i.e., the location of STAs and the AP as well as the characteristics of the multipath channel. In return, the radar processing will no longer be straightforward and the classical PWR processing applied on Orthogonal Frequency-Division Multiplexing (OFDM) modulated Wi-Fi

signals will not be reliable. Therefore, the PWR processing has to be adapted to take the precoder into account.

The literature is extensive on precoder-based active MIMO radar systems, where the precoder is explicitly designed to improve the MIMO system performance, see [5] and [6], and the references therein. In contrast, the literature is quite scarce when it comes to analyzing the impact of precoded signals on the passive radar processing. In [7], the authors explore the feasibility of reference signal reconstruction within the DVB-T2 framework, where the signals are potentially precoded. On the other hand, the authors in [8], [9], [10] investigate DVB-T based Multiple-Input Single-Output (MISO) passive radar systems without precoders. The goal of this paper is to analyze the issues raised by the precoded Wi-Fi signals, and propose possible solutions. Our contributions can be summarized as follows

- A system model which integrates the communication and passive radar functionalities is provided for a Multi-User Multiple-Input Single-Output (MU-MISO) system. Then, the surveillance signal is derived from the transmission of precoded Wi-Fi signals.
- We propose a single-antenna PWR scheme which aims at heuristically recovering the angle-of-departure (AoD) of the targets that are well-illuminated by the precoded Wi-Fi signals. To achieve this, the NDP is used to provide initial channel estimates. Then, during the MU-MIMO transmission, the corresponding cost function is minimized for a parameter space that is narrowed-down based on the initial estimates. Moreover, we also show that the Rician factor, also known as the K-factor, in the communication channel plays an important role on the recovery of AoDs.

This paper is structured as follows. In Section II, the system model for the communication and the PWR systems is provided. Also, the surveillance signal under the influence of precoder is derived. In Section III, we propose a method to exploit the precoded Wi-Fi signals in order to recover the AoD of potential targets. In Section IV, various numerical results are provided that assess the influence of precoder, as well as the estimation accuracy of the proposed method. Finally, the conclusion is drawn in Section V.

II. MU-MISO Model

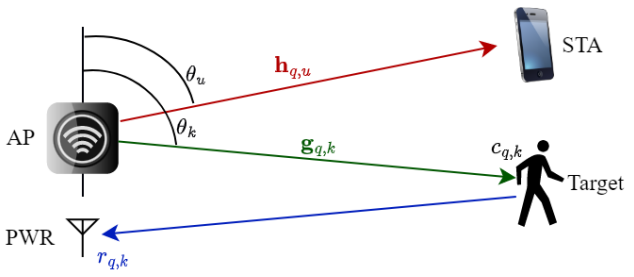

Fig. 1. The topography of the system.

In this section, we provide the system model for the scenario shown in Fig. 1. First, we detail the communication channel which is used to derive the precoder matrix per OFDM subcarrier q. Then, we switch our perspective to the PWR where the surveillance signal is derived for the kth target which is illuminated by the precoded Wi-Fi signal.

A. Communication Channel

Let us first define the one-way MISO communication channel perceived by the uth STA on subcarrier q as follows

$$\mathbf{h}_{q,u} = \begin{bmatrix} h_{q,u,1} & \dots & h_{q,u,n} & \dots & h_{q,u,N} \end{bmatrix}, \in \mathbb{C}^{1\times N}$$

where N is the number of transmitter (Tx) antennas at the AP, and U is the number of STAs. Each entry in $\mathbf{h}_{q,u}$ can be defined as

$$h_{q,u,n} = \sum_{l=0}^{L-1} \alpha_{l,u} e^{-j2\pi q \frac{\tau_{0,u}-\tau_{l,u}}{QT}} e^{-j\pi n \cos\theta_{l,u}}$$

where Q and T correspond to the number of subcarriers and the sampling interval, respectively. Moreover, l corresponds to the multipath component (MPC) index, and more specifically, $l = 0$ is the Line-of-Sight (LOS). The attenuation per path is modeled by $\alpha_{l,u}$, while the two cisoids model the phase per subcarrier due to the propagation delay $\tau_{l,u}$ and phase per antenna due to the angular spread $\theta_{l,u}$. Moreover, notice that L copies of a Wi-Fi frame arrive at an STA. If the LOS path dominates other MPCs, each STA will be synchronized with respect to the Wi-Fi frame that propagated through the LOS path. Hence, the first cisoid models the fading due to the MPCs relative to the LOS. Otherwise, the synchronization will occur based on the strongest MPC. For future reference, let us define the Rician K-factor as follows

$$\kappa_u = \frac{|\alpha_{0,u}|}{\sum_{l=1}^{L-1} |\alpha_{l,u}|}$$

which is the ratio between the amplitude of the LOS path and the remaining MPCs.

Once an STA obtains the Channel Transfer Function (CTF) per subcarrier, its singular value decomposition is computed, yielding

$$\mathbf{h}_{q,u} = \sigma_{q,u}\mathbf{b}^*_{q,u}$$

where $\mathbf{b}^*_{q,u}$ is the Hermitian transpose of $\mathbf{b}_{q,u}$ which is also known as the Beamforming Feedback Vector (BFV), and it contains the angular spread information per subcarrier from the AP to the considered STA. In order to obtain the precoder matrix, each STA sends $\mathbf{b}_{q,u}$ back to the AP. Once all the BFVs are collected by the AP, they are stacked on a matrix $\mathbf{B}_q$ and the Zero-Forcing Precoder $\mathbf{P}_q$ is computed for each subcarrier as follows

$$\mathbf{B}_q = [\mathbf{b}_{q,1}\ \mathbf{b}_{q,2}\ \dots\ \mathbf{b}_{q,U}], \in \mathbb{C}^{N\times U}$$
$$\mathbf{P}_q = \mathbf{B}_q(\mathbf{B}^*_q\mathbf{B}_q)^{-1}.$$

The Zero-Forcing Precoder can be seen as an orthogonalization procedure for all $\mathbf{b}_{q,u}$, such that inter-STA interference is minimized at each STA. Finally, the complex symbols that

will be transmitted over the antenna array at the AP take the following form

$$\mathbf{s}_q = \mathbf{P}_q \bar{\boldsymbol{s}}_q, \in \mathbb{C}^{N\times 1}$$

where $\bar{\boldsymbol{s}}_q = [\bar{s}_{q,1} \ \dots \ \bar{s}_{q,u} \ \dots \ \bar{s}_{q,U}]^T, \in \mathbb{C}^{U\times 1}$ contains the complex training/data symbols mapped on subcarrier q for user u. Notice that the precoder is designed to match only a specific set of channel coefficients: those of the STAs.

B. Radar Surveillance Signal with Precoding

Let us define the one-way MISO radar channel from the AP to the kth target as follows

$$\mathbf{g}_{q,k} = \begin{bmatrix} g_{q,k,1} & \dots & g_{q,k,n} & \dots & g_{q,k,N} \end{bmatrix}, \in \mathbb{C}^{1\times N}$$

whose entries are defined as

$$g_{q,k,n} = \sum_{l=0}^{L-1} \alpha_{l,k} e^{-j2\pi q \frac{\tau_{l,k}}{QT}} e^{-j\pi n \cos\theta_{l,k}}.$$

Since a target does not synchronize itself with respect to any one of the paths, each path, and its propagation delay are individually modeled by the first cisoid in the one-way radar channel. Similar to the communication channel, the second cisoid models the angular spread from the AP to the kth target.

Assuming that the K-factor for any target is relatively high –such that the LOS dominates all the other MPCs– the target channel coefficients can also be written as

$$\mathbf{g}_{q,k} = \lambda_{q,k} \mathbf{v}_k^*$$

where $\lambda_{q,k} = \alpha_k e^{-j2\pi q \frac{\tau_k}{QT}}$, $v_{k,n} = e^{-j\pi n \cos\theta_k}$, and we omit the index zero on α, τ and θ which corresponds to the LOS path. Then, the precoded Wi-Fi signal that illuminates the kth target can be defined as follows

$$c_{q,k} = \mathbf{g}_{q,k} \mathbf{s}_q$$

Assuming that the kth target is sufficiently illuminated, i.e., it is not aligned with the nulls of the precoded Wi-Fi transmission, and reflection has occurred, the PWR device –which is co-located with the AP– receives the following signal

$$\begin{aligned} r_{q,k} &= \alpha'_k e^{-j2\pi q \frac{\tau_k}{QT}} c_{q,k} + z_q \\ &= \beta_k e^{-j2\pi q \frac{2\tau_k}{QT}} \mathbf{v}_k^* \mathbf{s}_q + z_q. \end{aligned} \tag{1}$$

where z_q is the Additive White Gaussian Noise on subcarrier q. On the first line, α'_k and the additional cisoid model the one-way attenuation and the propagation delay from the target to the PWR, respectively. The second line shows the received signal more explicitly: i) the two-way attenuation β_k that is constant over subcarriers; ii) the two-way phase shift –modeled by the cisoid– varying over the subcarriers; iii) the angular spread between the AP and the target $\mathbf{v}_k^*$, and iv) the precoded signal $\mathbf{s}_q$. As mentioned earlier, the precoded signal is designed to match only some specific users, i.e., specific $\mathbf{b}_{q,u}^*$ vectors. Therefore, the combination between $\mathbf{v}_k^*$ and $\mathbf{s}_q$ will not be simplified if a target and a user are not aligned. In such a case, the phase due to propagation delay will be distorted by the angular spread and the precoded signal. In other words, $\mathbf{v}_k^* \mathbf{s}_q$ will act as a source of multiplicative interference that distorts each subcarrier differently depending on θ_k, and in some cases $\mathbf{v}_k^* \mathbf{s}_q$ can be close to zero, meaning that the kth target is not illuminated at all.

C. Radar surveillance signal in matrix form

Let us first define the following compact phase terms

$$d_k = e^{-j2\pi \frac{2\tau_k}{QT}}$$
$$v_k = e^{-j\pi \cos\theta_k}$$

where d_k and v_k model the fundamental phase due to the propagation delay and angular spread of the kth target, respectively. Moreover, notice that raising d_k and v_k to the power of q and n, respectively, yields the phase on the qth subcarrier and nth antenna, i.e., $d_k^q = e^{-j2\pi q \frac{2\tau_k}{QT}}$ and $v_k^n = e^{-j\pi n \cos\theta_k}$. Let us define the amplitude-delay vector as follows

$$\mathbf{d}_q = \begin{bmatrix} \beta_1 d_1^q & \beta_2 d_2^q & \dots & \beta_K d_K^q \end{bmatrix}^T, \in \mathbb{C}^{K\times 1}$$

whose kth entry corresponds to the attenuated phase-shift due to the propagation delay of the kth target on subcarrier q. The angular spread matrix is defined as follows

$$\mathbf{V} = \begin{bmatrix} v_1^1 & v_1^2 & \dots & v_1^N \\ v_2^1 & v_2^2 & \dots & v_2^N \\ \vdots & \vdots & \ddots & \vdots \\ v_K^1 & v_K^2 & \dots & v_K^N \end{bmatrix} = \begin{bmatrix} \mathbf{v}_1 \\ \mathbf{v}_2 \\ \vdots \\ \mathbf{v}_K \end{bmatrix}, \in \mathbb{C}^{K\times N}$$

whose rows correspond to the angular spread between the AP and the kth target, while its columns correspond to different antennas at the AP. Similarly, the precoded Wi-Fi signal per subcarrier can be arranged in the following form

$$\mathbf{s}_q = \begin{bmatrix} s_{q,1} & s_{q,2} & \dots & s_{q,N} \end{bmatrix}^T, \in \mathbb{C}^{N\times 1}$$

whose entries correspond to the complex symbols to be transmitted by the AP. Notice that both the $\mathbf{d}_q$ and $\mathbf{s}_q$ depend on the subcarrier index. However, the first one is associated with the radar channel, while the latter one is associated with the communication channel. Therefore, the angular spread matrix –which does not vary as a function of the subcarrier index– acts as the bridge between these two channels: from the complex symbols transmitted by the AP to the targets and back to the PWR. Finally, the surveillance signal received on subcarrier q is defined as follows

$$r_q = \mathbf{d}_q^T \mathbf{V} \mathbf{s}_q + z_q. \tag{2}$$

III. Estimation of Radar Parameters from Precoded Wi-Fi Signals

In this section, we propose the scheme shown in Fig. 2 which exploits the precoded Wi-Fi signals for PWR processing. To do so, the PWR obtains the initial amplitude-delay estimates based on the priorly known NDP during the CSS. When the STAs transmit back their BFVs, the PWR sniffs them to reconstruct $\mathbf{s}_q$. Finally, when the precoded signal transmission starts, the AoD of the well-illuminated targets is estimated.

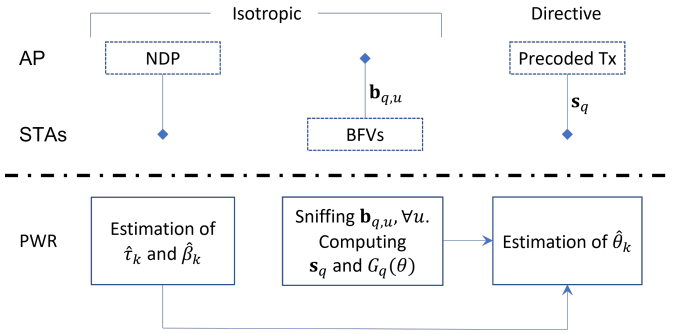

Fig. 2. The PWR processing stages in parallel with the Wi-Fi communication system.

A. Parameter estimation during the isotropic session

Let us define the surveillance signal corresponding to all the targets, obtained during the CSS session, i.e., without precoding, as follows

$$r_q^{iso} = \sum_k \beta_k e^{-j2\pi q \frac{2\tau_k}{QT}} \bar{s}_q + z_q$$

where $\bar{s}_q$ is the training symbol mapped on subcarrier q. Notice that the received signal contains the channel coefficients corresponding to the kth target without any distortions introduced due to the precoder. Therefore, the CTF per subcarrier can easily be estimated as follows

$$\hat{\rho}_q = \frac{r_q^{iso}}{\bar{s}_k} = \sum_k \beta_k e^{-j2\pi q \frac{2\tau_k}{QT}} + \frac{z_k}{\bar{s}_k}. \tag{3}$$

Here, $\hat{\rho}_q$ can be used as an initial channel measurement. By using the MUSIC algorithm [11], we can estimate the number of unique propagation delays K together with the delays themselves τ_k. To do so, the sample covariance matrix and its singular value decomposition are defined as follows

$$\mathbf{R}_\rho = \frac{1}{Q}\hat{\boldsymbol{\rho}}^*\hat{\boldsymbol{\rho}} = \begin{bmatrix}\mathbf{U}_s & \mathbf{U}_n\end{bmatrix}\begin{bmatrix}\boldsymbol{\lambda}_s & \mathbf{0}\\ \mathbf{0} & \boldsymbol{\lambda}_n\end{bmatrix}\begin{bmatrix}\boldsymbol{\mathcal{V}}_s^* & \boldsymbol{\mathcal{V}}_n^*\end{bmatrix}$$

where the CTF matrix is defined as $\hat{\boldsymbol{\rho}} = [\rho_1 \ \rho_2 \ \dots \ \rho_Q]$. Moreover, $\mathbf{U}_s$ and $\mathbf{U}_n$ correspond to the eigenvectors that span the signal and noise subspaces, respectively, while the entries in the diagonal matrices $\boldsymbol{\lambda}_s$ and $\boldsymbol{\lambda}_n$ are the associated eigenvalues. Let us define the search vector at a given propagation delay as follows

$$\mathbf{f}_\tau = \left[e^{-j2\pi\frac{\tau}{QT}} \ e^{-j2\pi 2\frac{\tau}{QT}} \ \dots \ e^{-j2\pi(Q-1)\frac{\tau}{QT}}\right]^T, \in \mathbb{C}^{Q\times 1}.$$

Finally, the MUSIC spectrum is obtained by solving the following cost function at the desired propagation delay values

$$J(\tau) = \frac{1}{\mathbf{f}_\tau^*\mathbf{U}_n\mathbf{U}_n^*\mathbf{f}_\tau}.$$

Detecting the peaks from the music spectrum $J(\tau)$ yields the unique propagation delay estimates $\hat{\tau}_k$. Then, the following system of equations can be written

$$\begin{bmatrix}\hat{\rho}_1\\ \hat{\rho}_2\\ \vdots\\ \hat{\rho}_Q\end{bmatrix} = \begin{bmatrix}\hat{d}_1 & \dots & \hat{d}_K\\ \hat{d}_1^2 & \dots & \hat{d}_K^2\\ \vdots & \ddots & \vdots\\ \hat{d}_1^Q & \dots & \hat{d}_K^Q\end{bmatrix}\begin{bmatrix}\beta_1\\ \beta_2\\ \dots\\ \beta_K\end{bmatrix} \tag{4}$$
$$\hat{\boldsymbol{\rho}} = \hat{\mathbf{D}}\boldsymbol{\beta}$$

where $\hat{d}_k^q = e^{-j2\pi q\frac{2\hat{\tau}_k}{QT}}$ which can be solved for $\boldsymbol{\beta}$ through Least Squares as follows

$$\hat{\boldsymbol{\beta}} = \hat{\mathbf{D}}^+\boldsymbol{\rho}$$

where $\hat{\mathbf{D}}^+$ is the pseudo-inverse of $\hat{\mathbf{D}}$ which is constructed based on $\hat{\tau}_k$. Hence, the first step is concluded where the set of amplitude-delay pairs, $(\hat{\beta}, \hat{\tau})_k$, are estimated by the PWR and the corresponding amplitude-delay vector can be constructed as follows [11]

$$\hat{\mathbf{d}}_q = [\hat{\beta}_1\hat{d}_1^q \ \dots \ \hat{\beta}_K\hat{d}_K^q]^T$$

B. Sniffing the Beamforming Feedback Vectors and Obtaining the Radiation Pattern

During the second part of the scheme, PWR simply acts as a physical layer sniffer, which collects the BFVs transmitted by the STAs to the AP. Therefore, based on these BFVs, the PWR can construct the same precoder matrix as the AP. Since every Wi-Fi packet includes training symbols, a part of the precoded Wi-Fi signal can be completely reconstructed, which we keep denoting as $\mathbf{s}_q$. Finally, the radiation pattern of the precoded signal transmitted per subcarrier can be computed for each AoD ϕ [12] as follows

$$G_q(\phi) = 4\pi\frac{|\mathbf{s}_q^*\mathbf{v}(\phi)|^2}{\int_\Omega |\mathbf{s}_q^*\mathbf{v}(\phi)|^2 d\Omega}, \phi \in \left[\frac{-\pi}{2}, \frac{\pi}{2}\right] \tag{5}$$

where Ω corresponds to the 4π steradian and $\mathbf{v}(\phi) = [e^{-j\pi\cos\phi} \ \dots \ e^{-jN\pi\cos\phi}]^T, \in \mathbb{C}^{N\times 1}$ is the steering vector at ϕ.

C. Parameter estimation during the directive session

When the AP starts the precoded signal transmission, AoD of the targets directly affects the surveillance signal power through $\mathbf{V}\mathbf{s}_q$ in (2). In other words, $\mathbf{V}\mathbf{s}_q$ can yield any value between 0 and $\sqrt{N}$ depending on: i) $\theta_{l,u}$ and θ_k; ii) subcarrier index q; iii) the K-factor in the communication channel, and iv) the size of Tx array N. The first two parameters are clearly related through the scenario topography. In other words, if the targets and the STAs are aligned, then $\mathbf{V}\mathbf{s}_q$ will yield relatively higher values, hence, the received signal energy will be mainly affected by the pathloss. Moreover, there will be a dependence on the subcarrier index q, since different subcarriers experience different levels of fading. On the other hand, K-factor in the communication channel plays a crucial role which is visualized in Fig. 3. When the K-factor is low, i.e., the LOS path does not dominate the MPCs or it does not even exist, the precoder

will make use of the multipath directions. This will yield a radiation pattern that is more uniformly distributed over all angles since the AP will exploit multiple directions. On the other hand, a high K-factor means that most of the energy will be focused towards the LOS direction while computing the precoder [4]. Therefore, the radiation pattern at the AP will contain U number of beams formed towards the STAs and sidelobes with significantly lower energy compared to the beams. In such a case, the radar coverage will be highly reduced, and the only parts of the scene that can reliably be covered by the PWR are the ones toward those beams. In both cases, N also plays an important role since it determines the beamwidth, sidelobe energy as well as nulls.

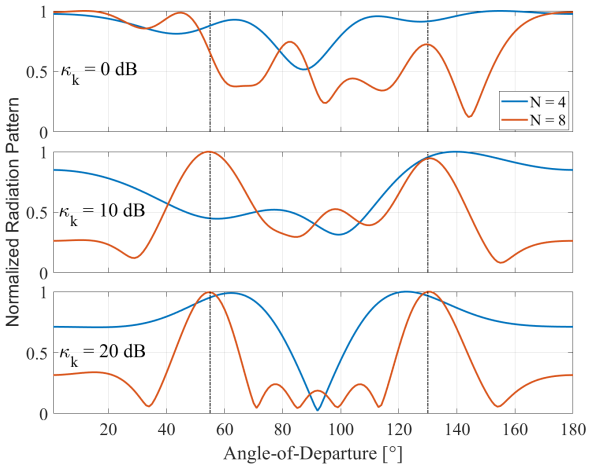

Fig. 3. Example radiation patterns as a function of ϕ and N while there are two STAs at 55° and 130°. For smaller K-factors, the radiation pattern is more uniformly distributed, i.e., there are no clear beams. For larger K-factors, the beams become clear meaning that the precoder is focusing most of the energy towards the LOS direction. Having more Tx antennas decreases the beamwidth and yields smaller sidelobes.

Based on the radiation pattern given in (5), let us define the following set of AoD angles per subcarrier q

$$\hat{\phi}_q = \{\phi \in [-\frac{\pi}{2}, \frac{\pi}{2}], G_q(\phi) \geq \mathcal{T}, q = 1, \ldots, Q\} \quad (6)$$

In words, each set $\hat{\phi}_q$ contains the AoD angles on which the energy of the radiation pattern is greater than the threshold $\mathcal{T}$ for the given subcarrier. The role of this threshold is to determine the angles on which the PWR device should look at. Therefore, it mainly depends on the directivity of the radiation pattern, i.e., the K-factor. Once we obtain the angle search space, we exhaustively search for the solution of the following discrete optimization problem

$$\arg\min_{\theta \in \hat{\phi}_q} \quad \sum_q \left\| r_q - \hat{\mathbf{d}}_q^T \mathbf{V}_\theta \mathbf{s}_q \right\|_2 \quad (7)$$

where θ is the angles in the set $\hat{\phi}_q$ for a given q, r_q is the measured surveillance signal defined in (2), and $\hat{\mathbf{d}}_q$ is the amplitude-delay vector formed during the isotropic transmission based on the estimates of $\hat{\tau}_k$ and $\hat{\beta}_k$. Notice that we limit the exhaustive search to i) only a few delay and amplitude values on which we are sure that there is a target, and ii) a subset of AoD values on which we are sure that the AP sufficiently illuminates.

This method also implies that a PWR equipped with a single antenna can either estimate the AoD of all the targets when the K-factor is low or some of the targets when the K-factor is high. In other words, in the best-case scenario, PWR can detect the range and AoD of all targets. In the worst-case scenario, PWR can detect only the targets that are in the vicinity of STAs. On the other hand, note that the optimization problem is solved heuristically, through exhaustive search. Given that the parameter search spaces are narrowed down, the exhaustive search can be sufficient enough without compromising the computational complexity. However, more elegant approaches, such as stochastic gradient descent with momentum [13], can solve the optimization problem more efficiently while potentially compromising the parameter estimation accuracy.

Moreover, let us further discuss the impact of $\mathcal{T}$ on the detection performance. When the K-factor is low, setting $\mathcal{T}$ to a high value means that there will be miss detections while setting it to a low value will allow PWR to detect the AoD of the targets. When the K-factor is high, the only detectable AoDs are the ones in the vicinity of STAs, i.e., towards the beams. Therefore, setting $\mathcal{T}$ to a lower value will not change the detection performance. Instead, it will just increase the size of the parameter space by including the AoDs which are not sufficiently illuminated.

IV. Numerical Analyses

In this section, numerical results are provided to show the accuracy achieved with the proposed scheme. Since we are specifically considering the Wi-Fi 802.11ax signals, our simulation parameters are adjusted to be fully compliant with the standard, and they are summarized in Table I. A few notes on these parameters: i) the number of subcarriers Q is directly linked to the signal bandwidth, such that when $Q = 256$, $B = 20$ MHz; ii) Radar Cross Section of humans ($\text{RCS}_{\text{human}}$) is fixed at -4 dBsm, and iii) the Tx/Rx antenna gains are the ones corresponding to the individual antennas. In all of our remaining analyses, we assume that there are two STAs, each equipped with a single antenna.

TABLE I
Summary of the Simulation Parameters

Parameter	Value	Unit	Parameter	Value	Unit
N	4, 8		$\text{RCS}_{\text{human}}$	-4	dBsm
Q	256, 1024		P_{Tx}	20	dBm
B	20, 80	MHz	$\text{G}_{\text{Tx/Rx}}$	1.2	dBi

In Fig. 4, we show the delay, amplitude, and AoD estimation accuracy in terms of Root Mean Square Error (RMSE) for two different subcarrier sizes, i.e., bandwidths, as a function of SNR. Note that each one of these parameters is estimated with different algorithms: delay with MUSIC, amplitude with least squares, and AoD by solving the optimization problem given in (7). More importantly, each estimation output on a given layer is an input to the next layer.

When SNR is lower than 10 dB, the delay estimation is quite inaccurate. Therefore, the amplitude estimation is also erroneous since least squares is solved for inaccurate delays. However, the delay estimation becomes more and more accurate as SNR improves, which provides better amplitude estimates in return. In all cases, wider bandwidths provide better estimation accuracy, which is more pronounced when SNR is poor. The AoD estimation accuracy follows a trend similar to delay and amplitude terms: it improves as SNR improves. However, we remind that the AoD estimation accuracy depends on the K-factor between the AP and each STAs. Thanks to the narrowed-down search space, the proposed scheme estimates only the AoDs of well-illuminated targets. Hence, the overall RMSE improves since the AoD of the poorly illuminated targets are not estimated at all.

In order to further analyze the AoD estimation accuracy, we provide the results shown in Fig. 5. In this case, the AoD search space is not narrowed down. Instead, the AoD estimation accuracy is evaluated for a target whose AoD varies from 0° and 180° while its range is fixed to provide 10 dB SNR. Notice that when $\kappa_k = 0$ dB, the AoD is accurately estimated regardless of the target position. The reason is that the AP exploits multiple AoDs in its precoder, i.e., it provides better coverage for the PWR processing. However, when $\kappa_k = 20$ dB, the AP focuses most of the energy on the direction of the LOS paths. Therefore, a reliable AoD estimation is possible only in the vicinity of the STAs, since anywhere else the signal energy $\mathbf{v}_k^* \mathbf{s}_q$ is quite low. Finally, for a larger array, e.g., $N = 8$, the beamwidth per STA decreases, and a smaller area is well-illuminated by the AP. Therefore, the set of angles where reliable AoD estimation is possible decreases as N increases.

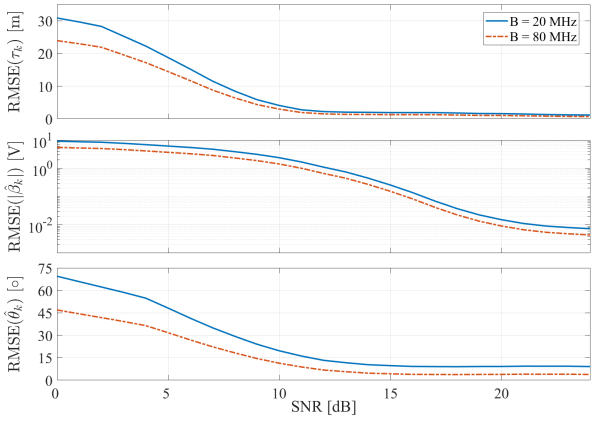

Fig. 4. From top to bottom, delay, amplitude and AoD estimation accuracy are shown, respectively. For each realization, delay and AoD parameters of the STAs and targets are randomized.

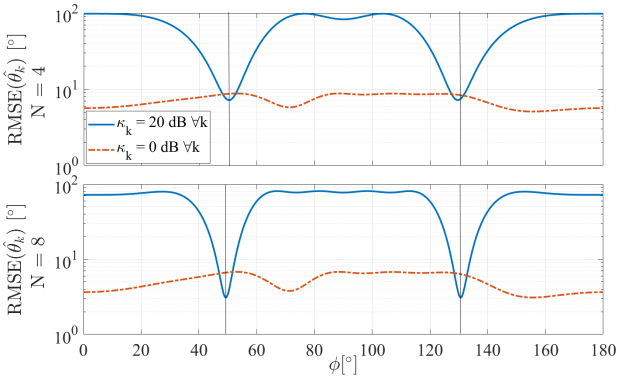

Fig. 5. RMSE over the angular spectrum when the STAs are at 50° and 130° AoDs with respect to the AP, and target AoD varies.

V. Conclusion

In this paper, we have shown that the MU-MIMO precoded Wi-Fi signals raise a significant concern for reliable PWR processing. By exploiting the synchronization scheme incorporated in the Wi-Fi system, we proposed a preliminary three-step-scheme where the amplitude-delay parameters of all the present targets are estimated during the CSS. Then, the AoDs are estimated during the precoded signal transmission only for the sufficiently illuminated targets. However, we emphasize that using more elegant approaches while solving the optimization problem may increase the accuracy of the scheme.

References

[1] F. Colone, et al. "WiFi-based passive bistatic radar: Data processing schemes and experimental results." IEEE Transactions on Aerospace and Electronic Systems 48.2 (2012): 1061-1079.

[2] Aruba Networks, "White Paper 802.11ax", www.arubanetworks.com/assets/wp/WP_802.11AX.pdf

[3] H. C. Yildirim, L. Storrer, et. al, "Passive Radar based on 802.11ac Signals for Indoor Object Detection," 2019 16th European Radar Conference (EuRAD), 2019, pp. 153-156.

[4] H. C. Yildirim, L. Storrer, et. al "Impact of MU-MIMO on Passive Wi-Fi Sensing: Threat or Opportunity?." 2022 2nd IEEE International Symposium on Joint Communications & Sensing (JC&S). IEEE, 2022.

[5] L. Zheng, M. Lops, et. al., "Radar and Communication Coexistence: An Overview: A Review of Recent Methods," in IEEE Signal Processing Magazine, vol. 36, no. 5, pp. 85-99, Sept. 2019, doi: 10.1109/MSP.2019.2907329.

[6] A. Babaei, W. H. Tranter, et. al., "A practical precoding approach for radar/communications spectrum sharing," 8th International Conference on Cognitive Radio Oriented Wireless Networks, 2013, pp. 13-18, doi: 10.1109/CROWNCom.2013.6636787.

[7] D. W. O'Hagan, M. Setsubi, et. al., "Signal reconstruction of DVB-T2 signals in passive radar," 2018 IEEE Radar Conference (RadarConf18), 2018, pp. 1111-1116, doi: 10.1109/RADAR.2018.8378717.

[8] M. Weis, "Group sparsity techniques for data fusion of a passive MISO radar network," 2016 17th International Radar Symposium (IRS), 2016, pp. 1-5, doi: 10.1109/IRS.2016.7497374.

[9] H. Wang, J. Yi, et. al., "Tracking Algorithm with Data Fusion in Single Frequency Network-based MISO Passive Radar," 2018 12th International Symposium on Antennas, Propagation and EM Theory (ISAPE), 2018, pp. 1-3, doi: 10.1109/ISAPE.2018.8634332.

[10] M. M. Chitgarha, M. N. Majd, et. al., "Choosing the position of the receiver in a MISO passive radar system," 2012 9th European Radar Conference, 2012, pp. 318-321.

[11] P. Stoica, RL. Moses, "Spectral analysis of signals", Upper Saddle River, NJ: Pearson Prentice Hall; 2005 May.

[12] A. Constantine Balanis, "Antenna theory: analysis and design", John wiley & sons, 2015.

[13] Y. Liu, Y. Gao, W. Yin, "An improved analysis of stochastic gradient descent with momentum", Advances in Neural Information Processing Systems. 2020;33:18261-71.